Colloid Polym Sci 273:653–660 (1995)

ORIGINAL CONTRIBUTION

R. Mutter
B. Stühn

Microphase separation transition and ordering kinetics in thin films of diblock copolymers

Received: 28 December 1994
Accepted: 6 March 1995

R. Mutter · Dr. B. Stühn (✉)
Fakultät für Physik und
Materialforschungszentrum
Hermann-Herder-Straße 3
79104 Freiburg, FRG

Abstract Using x-ray reflectivity measurements, we have investigated the structure of films of a symmetric diblock copolymer of polystyrene-b-polyisoprene ($M_w = 15\,700$). The film thickness is in the range of 1 μm. In equilibrium the films consist of lamellae with a thickness of 15.3 nm. They are nearly completely oriented parallel to the substrate. The evolution of oriented structure is studied by time-dependent experiments. The time constants of the structure formation depend strongly on the annealing temperature. An enhancement of the diffuse intensity in the range of Yoneda scattering is evidence for an additional surface structure.

Key words Block copolymers – thin films – microphase separation transition – x-ray reflection ordering kinetics

Introduction

Symmetric diblock copolymers are macromolecules consisting of two different homopolymers connected by a covalent bond. The temperature-dependent phase behavior of such polymers in bulk samples is theoretically treated in a fundamental work by Leibler [1]. For polymers of symmetric composition a lamellar phase is expected in the ordered state. Experimental results confirm these predictions [2]. For films of a diblock copolymer the interfaces affect the behavior of the polymer due to the different surface tensions of the two blocks. Theory predicts an oscillatory decaying composition variation, even for temperatures in the disordered state [3].

In thin films of symmetric diblock copolymers with a film thickness on the order of the lamellar thickness, the film structure is determined by the competition of the two lengths. In general, the film thickness is a non integral multiple of the lamellar thickness and, consequently, the equilibrium structure of the film consists of lamellae oriented parallel to the substrate and an incomplete top layer [4]. The temperature of the phase transition in these films is elevated compared to the bulk. This means the ordered phase is stabilized by the interfaces. The time constants for the formation of the ordered structure correspond to the formation of long-range order in the bulk of the same polymer.

The present work focuses on the structure formation in films of a symmetric diblock copolymer with a thickness on the order of magnitude of about 1 μm corresponding to a stacking height of 50–70 lamellae. With x-ray reflectivity measurements we have investigated the film structure in the direction perpendicular to the surface. Taking diffuse scattering into account, in addition to the specularly reflected intensity, also information about the lateral structure can be obtained. With time-dependent measurements the formation of the oriented structure can be observed.

Experimental section

Sample description

The polystyrene/polyisoprene diblock copolymer used in this study is the same as the one in refs. [4, 5]. Its molecu-

lar weight is 15 700 and the polydispersity $M_W/M_N = 1.04$. The volume fraction of polystyrene has been determined with NMR to be $f = 0.44$. The ordered state is of lamellar symmetry and the bulk lamellar thickness is 16.2 nm. The phase transition temperature in the bulk was determined using small-angle x-ray scattering (SAXS) and measurements of the dynamic shear modulus G^*. It was consistently found to be $T_{MST} = 362\,\text{K}(\pm 2)$ [5]. Films of the block copolymer were prepared by dissolving it in toluene and spin-coating the solution onto microscope slides. The concentration of the solution was in the range of 20%.

X-ray reflectivity set-up

The experimental set-up used for the x-ray reflectivity measurements is shown in Fig. 1. It consists of a Kratky compact camera modified for the reflection experiments. The x-ray source is a rotating anode generator (A) with a copper anode. The wavelength of the used CuK_α-radiation is $\lambda = 0.1542$ nm. S denotes the sample table with a size of 35 mm × 33 mm. The sample can be heated from room temperature to about 180 °C with a stability of ± 0.1 K. The angle between the incoming beam and the sample θ can be varied by a stepping motor in steps of 0.0175 mrad. K denotes the Kratky collimating system of the camera. The reflected beam is monochromized by a graphite crystal (M) and its intensity is registered with a scintillation counter. The detector D with the detector slit DS (angle 2θ) can be varied with an angular resolution of 0.025 mrad. For a fixed position of the sample the detector unit is scanned through 2θ for the registration of the reflected beam and the background. Figure 2 shows such a scan. The background is determined from this measurement as the flat intensity on both sides of the peak (see Fig. 2). The reflectivity is calculated by dividing the integral intensity of the peak after the subtraction of the background by the intensity of the primary beam. The angular position of the sample θ is determined by taking half the scattering angle as given by the center of the reflected beam. In the range of high and total reflectivity at low angles θ the primary beam is attenuated by aluminum plates. The attenuation factors are determined separately

Fig. 1 Schematic drawing of the experimental setup used for the x-ray reflectivity measurements

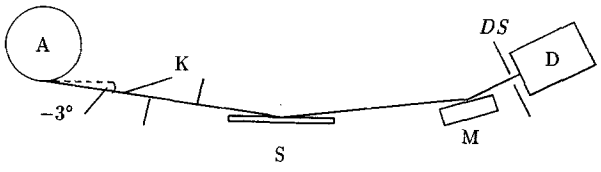

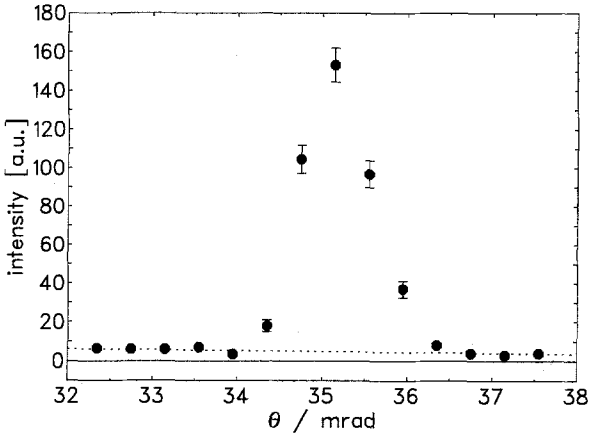

Fig. 2 2θ-scan of the reflected beam and background scattering (broken line)

and are kept fixed for the whole measurements. The attenuators are located in front of the collimating system of the camera and can be put into the beam automatically. With this set-up it is possible to measure the reflectivity automatically over six decades.

Two examples of reflectivity measurements are given in Fig. 3. In both cases the sample was a film of the block copolymer on a glass substrate. Figure 3a shows a characteristic oscillation in the data due to the interference of the radiation reflected at the substrate-film and the film-vacuum interface of the film (Kiessig fringes [6]). The period of the oscillation is only determined by the thickness of the

Fig. 3 Reflectivity measurements of films of a symmetric diblock copolymer. For ultrathin films (a) the thickness can be determined directly by the period of the Kiessig fringes. For thicker films (b) the thickness can be determined by the absorption of the x-ray beam in the film

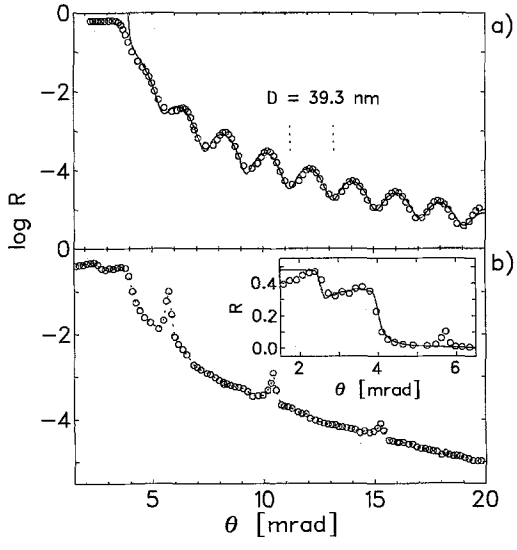

film. Consequently, this technique provides a good method to determine the thickness of films in the range of 1–100 nm. For thicker films (Fig. 3b) the Kiessig oscillation cannot be resolved due to the resolution of the camera. The structure in the reflectivity curve here is given by scattering from internal structures. In the case of thick films, however, the thickness can be determined by the absorption of the x-ray beam in the film for low angles of incidence. The inset in Fig. 3b shows the reflectivity in the range of total reflection on a linear scale. Steps can be seen at the critical angle of the film θ_{cf} and of the substrate θ_{cs}. For angles $\theta < \theta_{cf}$ the x-ray beam is totally reflected at the film-vacuum interface. For angles $\theta_{cf} < \theta < \theta_{cs}$ the radiation penetrates into the film but is totally reflected at the film-substrate interface. For thick films the attenuation of the radiation by absorption in the film cannot be neglected and leads to a decrease of the reflectivity. With the known mass absorption coefficients of the film, the thickness can be calculated from the height of these steps. For the measurement shown in Fig. 3b, one obtains a thickness of approximately 1 μm.

Principles of x-ray reflectivity

In this section, we briefly recall the concept of x-ray reflectivity and collect the formulae necessary for the subsequent interpretation of data. A detailed description of the principles of the x-ray reflectivity technique is given in the literature [7, 8]. The reflection of x-rays at surfaces and interfaces can be treated as the reflection of light with wavelengths in the visible range. For a fixed wavelength in the x-ray range all properties of the surface or a thin film are described by the refractive index $n(z)$ with

$$n = 1 - \delta + \imath\beta \tag{1}$$

and z the direction perpendicular to the surface. The imaginary part β describes absorption effects, the real part δ is

$$\delta(z) \sim \lambda^2 \rho_e(z) \tag{2}$$

with the wavelength λ of the x-ray radiation and the electron density $\rho_e(z)$ in z-direction. For an ideal surface, i.e., $\rho_e(z) = \rho_0 \cdot \Theta(z)$ with the Heaviside step function $\Theta(z)$, the reflectivity can be calculated exactly (Fresnel reflectivity)

$$R_F = \left| \frac{k_{z,1} - k_{z,2}}{k_{z,1} + k_{z,2}} \right|^2 , \tag{3}$$

with $k_{z,i} = \frac{2\pi}{\lambda} n_i \sin\theta_i$. The subscript $i = 1, 2$ refers to vacuum and film, respectively. A variation of the ideal step structure results in an additional modulation factor of the reflectivity [9]. Within Born's approximation, i.e., at sufficiently small values of R, this factor is given as

$$R = R_F \cdot \left| \frac{1}{\rho_\infty} \int dz e^{iq_z z} \frac{\partial \rho_e(z)}{\partial z} \right|^2 . \tag{4}$$

Here, $q_z = \frac{4\pi}{\lambda} \sin\theta_1$ is the length of the scattering vector. This approximation, however, is only valid for $q \geqq 3\text{–}4 q_{cs}$ with q_{cs} corresponding to θ_{cs}. Internal refraction may be taken into account by replacing the z-component of the scattering vector q_z in the Fourier transform by the value in the film $\hat{q}_z$. For $\hat{q}_z$ follows

$$\hat{q}_z = \sqrt{q_z^2 - q_{c,f}^2} \tag{5}$$

with $q_{c,f}$ corresponding to $\theta_{c,f}$.

Discussion of results

In the following, we discuss the equilibrium structure of the block copolymer films and subsequently turn to the kinetics of structure formation as observed in time-resolved reflection experiments.

Equilibrium structure

In order to reach the equilibrium state the block copolymer films prepared by spin coating were annealed at a temperature only a few degrees below the microphase separation transition temperature T_{MST}. Figure 4 shows the reflectivity measurements before and after annealing. The reflectivity data before annealing show no structure; the Kiessig oscillation, due to interference effects at both interfaces, cannot be resolved. After annealing the data show Bragg peaks up to the fourth order. This additional scattering is an indication of the internal structure of the

Fig. 4 Reflectivity measurements of a film of a symmetric diblock copolymer before (●) and after (○) annealing

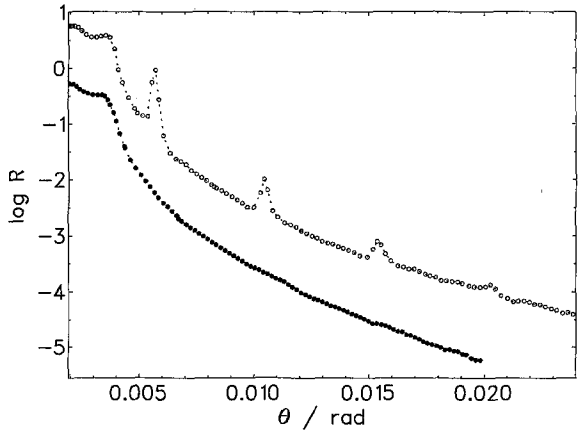

annealed film. To explain these data a model for the electron density has to be assumed. In the present case a completely ordered lamellar structure is adopted. The electron density in the direction perpendicular to the surface for that model is given by

$$\rho(z) = \rho_{fv}\, h(z, \sigma_f) + \mathrm{lam}(0, D) + (\rho_s - \rho_{fs})\, h(z - D, \sigma_s)\,. \quad (6)$$

$h(z, \sigma)$ denotes a error-functional step function with

$$h(z, \sigma) = \frac{1}{2} + \frac{1}{\sqrt{2\pi}\sigma}\int_0^z e^{-x^2/2\sigma^2} dx\,. \quad (7)$$

lam(0, D) denotes the lamellar structure of the film with

$$\mathrm{lam}(0, D) = \sum_{n=0}^{m} [l_1(z) * \delta(z - n d_{\mathrm{lam}})] \quad (8)$$

and

$$l_1(z) = \rho_1 + \Delta\rho \cdot h(z, \sigma_i) - \Delta\rho \cdot h(z - f d_{\mathrm{lam}}, \sigma_i) \quad (9)$$

the electron density for a single lamella as shown in Fig. 5. The convolution of $l_1(z)$ with a δ-function in Eq. (8) produces a periodic repetition of the electron density variation due to the lamellar structure. Here, d_{lam} denotes the thickness of the styrene-isoprene lamella, f is the fraction of the styrene component, and σ_i is the width of the transition zone between the two blocks, assuming an error-functional form for this range. $\Delta\rho = \rho_2 - \rho_1$ is the difference in the electron density of the two blocks of the polymer (cf. Fig. 5). ρ_{fv} and ρ_{fs} denote the densities of the first and last block respectively. σ_f and σ_s are the roughness parameters of the film and the substrate surface, ρ_s is the density of the substrate. In Born's approximation (Eq. (4)) the reflectivity is then given as

$$R(q_z) = \frac{R_F(q_z)}{\rho_s^2}\Big|\rho_f G(q_z, 1/\sigma_f) + \underbrace{\mathrm{FTR}\left[\frac{\partial}{\partial z}\mathrm{lam}(0, D)\right]}_{S_{\mathrm{lam}}(q_z)} + (\rho_s - \rho_f)\, e^{iq_z D}\, G(q_z, 1/\sigma_s)\Big|^2\,, \quad (10)$$

with $G(q_z, \sigma)$ a Gaussian with the width σ. The important feature of this reflectivity is the second term $s_{\mathrm{lam}}(q_z)$, the structure amplitude of the ordered lamellar structure. For a single lamella the structure amplitude is

$$s_1(q_z) = \mathrm{FTR}\left[\frac{\partial}{\partial z} l_1(z)\right] = \Delta\rho\; G(q_z, 1/\sigma_i)\,(1 - e^{iq_z f d_{\mathrm{lam}}})\,. \quad (11)$$

The structure of the complete film is given by Eq. (8) and for the structure amplitude of the complete film follows

$$s_{\mathrm{lam}}(q_z) = \mathrm{FTR}\left[\frac{\partial}{\partial z}\,\mathrm{lam}\,(0, D)\right] = \Delta\rho G(q_z, 1/\sigma_i)\,(1 - e^{-iq_z f d_{\mathrm{lam}}})\frac{e^{iq_z D_{\mathrm{film}}} - 1}{e^{iq_z D_{\mathrm{film}}} + 1}\,, \quad (12)$$

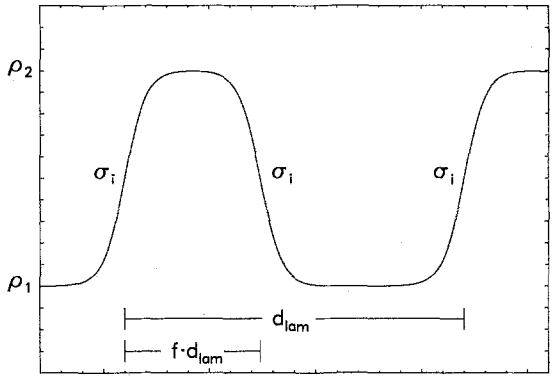

Fig. 5 Model of the electron density for a completely oriented lamellar structure

with $(m + 1)\, d_{\mathrm{lam}} = D_{\mathrm{film}}$. The first two terms represent the form factor of the lamellar structure, the last term describes the single peaks. With Eq. (10) the reflectivity can thus be calculated for the regime of validity of the Born approximation. Due to the thickness of the film the interference effects between the two surfaces and the lamellar structure cannot be resolved. We therefore seek a simplified expression for a fit of the observed reflection profiles. The essential structures of the reflectivity data are given by a smooth curve due to the rough interfaces, and the Bragg peaks due to the internal structure of the film, i.e. s^2_{lam}. In a simplified form the reflectivity is

$$R(q_z) = \frac{R_F(q_z)}{\rho_s^2}\,(G_0(q_z) + s^2_{\mathrm{lam}}(q_z))\,, \quad (13)$$

with G_0 including the whole information of the mean curve of the reflectivity. With the reflectivity $R_0(q_z)$ of a film with no internal structure the lamellar structure factor s^2_{lam} follows as

$$s^2_{\mathrm{lam}}(q_z) = \frac{R - R_0}{R_F}\cdot\rho_s^2\,. \quad (14)$$

The determination of the structure factor is thus possible by reference to different measurements of a film in its ordered and disordered states respectively. Figure 6 shows a fit of the lamellar structure factor (Eq. (11)) to the integral intensities of the Bragg peaks. The resulting parameters are

$\sigma_i = (1.2 \pm 0.1)$ nm

$f = 0.41 \pm 0.01$

$d_{\mathrm{lam}} = (15.3 \pm 0.2)$ nm

The low interface thickness σ_i confirms our assumption of complete orientation of the lamellae. A distortion of the lamellar order would result in an enhancement of the

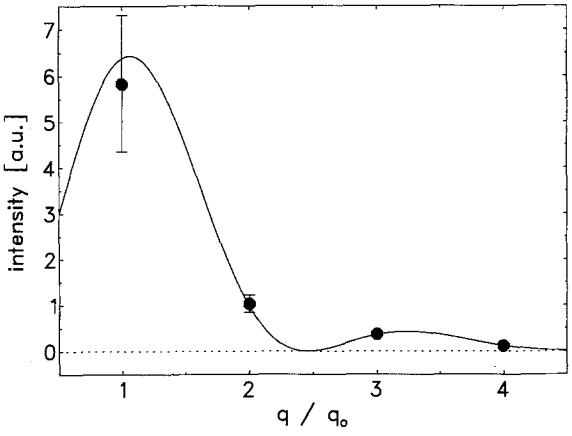

Fig. 6 Adjustment of the structure factor of the lamellar structure to the integral Bragg intensities

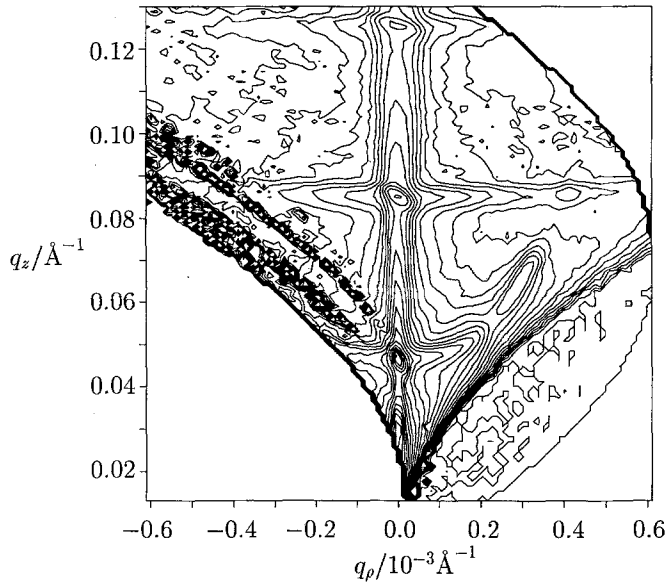

Fig. 7 Contour plot of specular and diffuse reflectivity of an oriented lamellar structure

interfacial thickness σ_i. For the lamellar thickness d_{lam} calculated from the peak position a smaller value results than from the bulk measurements.

Temperature dependence of the ordered structure

During a reflection measurement the angle of the sample surface varies between $\approx 1°$ and 3° relative to the horizontal. This causes a distortion of the lamellar order in the sample at higher temperatures as a result of the onset of flowing processes for temperatures $T > T_{gs}$ with T_{gs} the glass transition on temperature of the styrene component. DSC measurements show a glass transition temperature at about $T_{gs} \approx 50\,°\text{C}$. Due to this effect a determination of the stabilization of the ordered lamellar structure by the surfaces above T_{gs} is not quantitatively possible. The existence of a surface-induced order for temperatures above the microphase separation transition temperature as reported by Russell et al. [10], however, cannot be excluded.

Diffuse scattering

Additional information on the film structure may be derived from diffuse scattering. Data were recorded in 2θ-scans from constant values $2\theta_{\text{min}}$ to $2\theta_{\text{max}}$ for different values of the angle θ. Using

$$q_\rho = k \cdot (\cos(2\theta - \theta) - \cos\theta)$$

$$q_z = k \cdot (\sin(2\theta - \theta) + \sin\theta) \qquad (15)$$

the data were converted into the coordinates of the reciprocal space q_ρ and q_z with q_ρ denoting the scattering vector component parallel to the film surface. Figure 7 shows the reflectivity data in a contour plot in the range of specular and the diffuse scattering for a film with an oriented lamellar structure. The structure of the measured range results from the transformation of the data from the $\theta - 2\theta$-grid to the $q_\rho - q_z$-grid. The specular reflectivity, i.e., the intensity for $q_\rho \equiv 0$, shows the Bragg peaks to the third order resulting from the ordered lamellar structure. The extension of the Bragg peaks into the range of diffuse scattering is due to an incomplete orientation of the lamellae.

We emphasize the extremely small values of q_ρ as compared to q_z (see Fig. 6). This allows the observation of large scale lateral structure on the film surface [11].

An additional peak in the diffuse range can be seen at $q_\rho \approx 0.3 \cdot 10^{-3}\,\text{Å}^{-1}$ and $q_z \approx 0.06\,\text{Å}^{-1}$. This peak is an indication for the existence of lateral correlation in the electron density fluctuation. Its intensity is enhanced for angles $(2\theta - \theta)$ or θ in the range of θ_c, the critical angle of total reflection. The dimensions of these lateral structures are in the order of μm. Temperature-dependent rocking scans, i.e., θ-scans for constant 2θ are given in Fig. 8 in a cooling run. In addition to the peak of specular reflectivity an enhancement of the diffuse scattered intensity for angles $\theta = \theta_c$ (≈ 4 mrad) and $(2\theta - \theta) = \theta_c$ (≈ 16 mrad) (Yoneda-scattering [12]) is seen. When cooling down to room temperature the appearance of an additional peak well separated from the Yoneda scattering is clearly visible. The existence of the peak is obviously correlated to the lamellar structure in the film. The origin of this peak may be a lateral surface structure of islands and holes as has been already found in ultrathin films of symmetric block copolymers. Such structures may also exist in the bulk as tubular connections between lamellae.

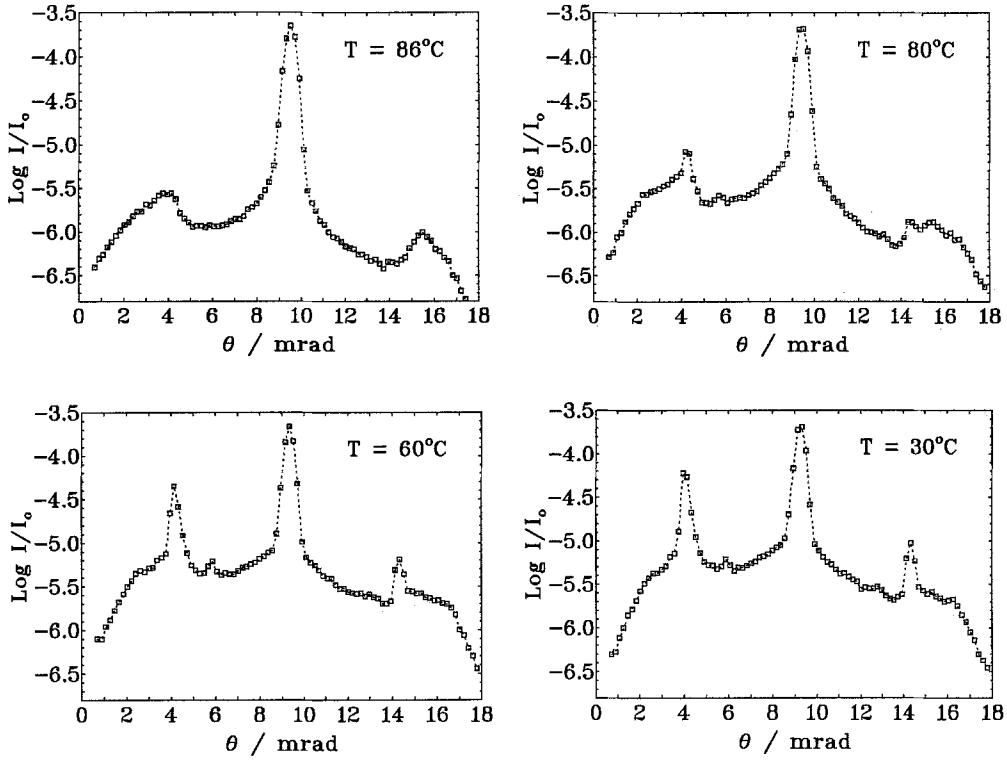

Fig. 8 Temperature-dependent rocking scan in a cooling run

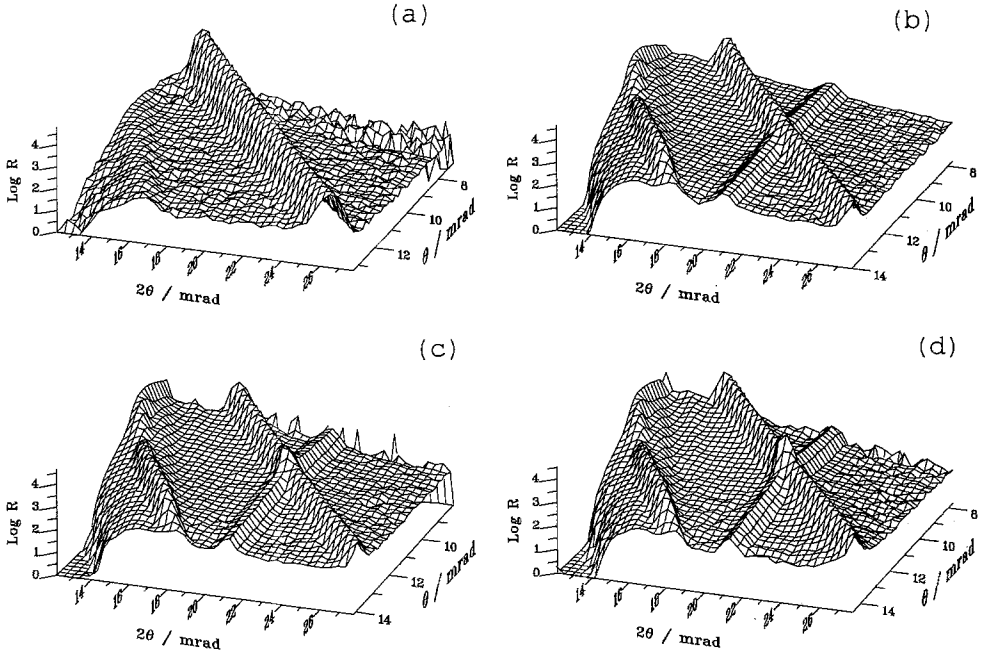

Fig. 9 Specular and diffuse reflectivity data after spin coating (a), and annealing times of 10 min (b), 20 min (c), and 40 min (d). The microphase separation transition takes place between (a) and (b). Orientational ordering is seen to proceed in (c) and (d)

Dynamics of the ordering

To characterize the dynamics of the ordering of the lamellae, time-dependent experiments were carried out. In order to avoid a destruction of the sample structure by the flowing of the polymer, the sample was kept at the annealing temperature T for a time Δt in a horizontal position and then rapidly cooled down to room temperature for the measurement. These steps were repeated several times. Figures 9a–d show the data after spin-coating and for

three annealing times. The annealing temperature for this experiment was $T = 85\,^{\circ}\mathrm{C}$. The data are recorded in a $\theta - 2\theta$ grid to get, as well, the specularly reflected beam as the diffuse scattering. The data of the sample immediately after preparation show only the specularly reflected beam on a flat diffuse background. After the first annealing step an additional scattering can be seen at constant $2\theta \approx 20$ mrad. This scattering is due to the lamellar structure of the microphase separated block copolymer. It corresponds to the second order Bragg peak in Fig. 4. In this first step the microphase separation is completed, but the lamellae are randomly oriented. Also, the peak in the diffuse range can be seen after the first annealing step. Further annealing (Fig. 9c, d) leads to an enhancement of the specular reflectivity in the range of the Bragg peak. This increase of intensity can be seen in detail in a q_z-scan (Fig. 10), i.e., the data for the condition $2\theta = 2 \cdot \theta$. The increasing intensity of the Bragg peak in the range of the specular reflectivity comparing to the isotropic scattering of the lamellar structure is caused by the orientation of the lamellae parallel to the substrate-film and the film-vacuum interfaces. The remaining intensity in the non-specular range is caused by a weak disorder of the lamellae. A determination of the film orientation distribution, however, is not possible because of the limited regime of accessible q_ρ. The additional scattering intensity in the range of specular reflectivity due to the lamellar ordering is determined by fitting a Gaussian to the peaks. The resulting temperature dependence is given in Fig. 11. It can phenomenologically be described by an Avrami equation,

$$I(t) = I_\infty \cdot \left(1 - \exp\left(-\frac{t}{\tau}\right)^n\right), \tag{16}$$

with an exponent $n = 3$. The time constants τ for three different temperatures are given in Table 1. Remarkable is

Fig. 10 q_z-scans in the range of specular reflectivity for different annealing times

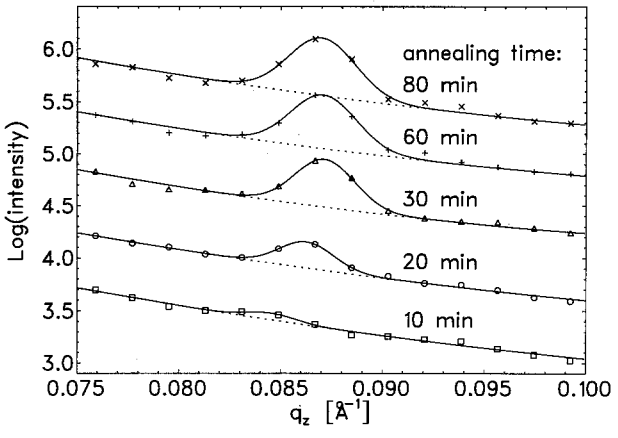

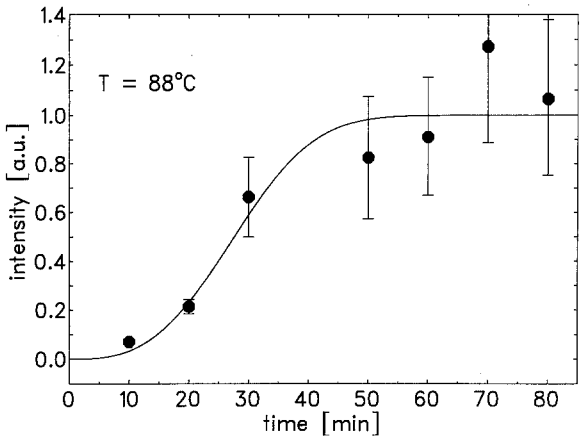

Fig. 11 Time dependence of the specular intensity from Fig.10

Table 1 Orientation times of the microphase separated lamellae for annealing temperatures just below T_{MST}

T [°C]	τ [min]
82	1030
85	210
88	31

the strong temperature dependence of the time constants. These times are considerably longer than the times found for the structure formation process in bulk [13] and in thin films [4] of the same diblock copolymer. Reorientation of the lamellae obviously is a separate process which proceeds after the microphase separation transition has taken place.

Conclusions

By annealing films of a symmetric blockcopolymer only a few degrees below the microphase transition temperature, one can achieve a nearly complete orientation of the lamellae parallel to the surfaces. This regular structure in the direction perpendicular to the surfaces may be determined by the analysis of the specular x-ray reflectivity. Taking the diffuse scattering into account an additional scattering due to a lateral structure can be observed. This lateral structure is coupled to the microphase separated lamellar structure. The evolution of the oriented structure can be observed in time-dependent measurements. For the temperatures chosen for these experiments the microphase separation transition proceeds in the first annealing step. The orientation of the lamellae in the further annealing steps can be observed by the enhancement of the intensity of the specular Bragg peaks.

Acknowledgment We are grateful to Prof. Dr. G. Strobl for continuous support and helpful discussions.

Colloid & Polymer Science, Vol. 273, No. 7 (1995)

References

1. Leibler L (1980) Macromolecules 13: 1602
2. Bates FS, Fredrickson GH (1990) Ann Rev Phys Chem 41: 525–557
3. Fredrickson GH (1987) Macromolecules 20:2535
4. Mutter R, Stühn B submitted to Macromolecules
5. Stühn B, Mutter R, Albrecht T (1992) Europhysics Letters 18(5):427
6. Kiessig H (1931) Ann d Phys 10, Nr. 7: 51
7. Russell TP (1990) Materials Science Reports Volume 5, pages 171–271. North Holland
8. Penfold J, Thomas RK (1990) J Phys: Condens Matter 2:1369–1412
9. Braslau A, Pershan PS, Swislow G, Ocko BM, Als-Nielsen J (1988) Phys Rev A 38:2457
10. Menelle A, Russell TP, Anastasiadis SH, Satija SK, Majkrzak CF (1992) Phys Rev Letters 68:67
11. Cai Z, Huang K, Montano PA, Russell TP, Bai JM, Zajac GW (1993) J Chem Phys 98:2376
12. Sinha SK, Sirota EB, Garoff S, Stanley HB (1988) Phys Rev B 38:2297
13. Stühn B, Vilesov A, Zachmann HG (1994) Macromolecules 27:3560